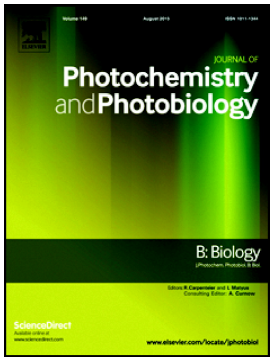

Photodynamic therapy of tumour cells mediated by the natural anthraquinone parietin and blue light

María Laura Mugas, Gustavo Calvo, Juliana Marioni, Mariela Céspedes, Florencia Martinez, Daniel Sáenz, Gabriela Di Venosa, José L. Cabrera, Susana Nuñez Montoya, Adriana Casas

PII: S1011-1344(20)30539-X

DOI: https://doi.org/10.1016/j.jphotobiol.2020.112089

Reference: JPB 112089

To appear in: *Journal of Photochemistry & Photobiology, B: Biology*

Received date: 11 September 2020

Revised date: 15 November 2020

Accepted date: 18 November 2020

Please cite this article as: M.L. Mugas, G. Calvo, J. Marioni, et al., Photodynamic therapy of tumour cells mediated by the natural anthraquinone parietin and blue light, *Journal of Photochemistry & Photobiology, B: Biology* (2020), https://doi.org/10.1016/j.jphotobiol.2020.112089

Photodynamic therapy of tumour cells mediated by the natural anthraquinone parietin and blue light

María Laura Mugas[1-2], Gustavo Calvo[1], Juliana Marioni[2], Mariela Céspedes[1], Florencia Martinez[3], Daniel Sáenz[1], Gabriela Di Venosa[1], José L. Cabrera[2-3], Susana Nuñez Montoya[2-3], Adriana Casas[1,*] **adriana@qb.fcen.uba.ar**

[1]Centro de Investigaciones sobre Porfirinas y Porfirias (CIPYP), CONICET and Hospital de Clínicas José de San Martín, Universidad de Buenos Aires, Ciudad de Buenos Aires, Argentina.

[2]Universidad Nacional de Córdoba, Facultad de Ciencias Químicas, Departamento de Ciencias Farmacéuticas. Haya de la Torre y Medina Allende, Ciudad Universitaria, Córdoba, Argentina.

[3]Consejo Nacional de Investigaciones Científicas y Técnicas (CONICET), Instituto Multidisciplinario de Biología Vegetal (IMBIV), Córdoba, Argentina.

[*]Corresponding author at: Centro de Investigaciones sobre Porfirinas y Porfirias (CIPYP), CONICET and Hospital de Clínicas José de San Martín, Universidad de Buenos Aires, Córdoba 2351 1er subsuelo, CP1120AAF Buenos Aires. Argentina

ABSTRACT

Photodynamic therapy (PDT) is a treatment for superficial tumours involving the administration of a photosensitiser followed by irradiation.

The potential of the natural anthraquinone parietin (PTN) in PDT is still relatively unexploited. In the present work, PTN isolated from the lichen *Teoloschistes nodulifer* (Nyl.) Hillman (Telochistaceae) was evaluated as a potential photosensitiser on tumour cells employing UVA-Vis and blue light.

Blue light of 2 J/cm^2 induced 50% death of K562 leukaemic cells treated 1 h with 30 µM PTN (Protocol *a*). Higher light doses (8 J/cm^2) were needed to achieve the same percentage of cell death employing lower PTN concentrations (3 µM) and higher exposure times (24 h) (Protocol *b*). Cell cycle analysis after both protocols of PTN-PDT revealed a high percentage of sub-G1 cells. PTN was found to be taken up by K562 cells mainly by passive diffusion.

Other tumour cells such as ovary cancer IGROV-1 and LM2 mammary carcinoma, as well as the normal keratinocytes HaCaT, were also photosensitised with PTN-PDT.
We conclude that PTN is a promising photosensitiser for PDT of superficial malignancies and purging of leukaemic cells, when illuminated with blue light. Thus, this light wavelength is proposed to replace the Vis-UVA lamps generally employed for the photosensitisation of anthraquinones.

Keywords: tumour cells, leukaemia, natural anthraquinone, blue light, photosensitiser, photodynamic therapy.

Abbreviations:

PDT	photodynamic therapy
PS	photosensitizer
AQ/AQs	Anthraquinone/s
PTN	parietin
DMSO	dimethyl sulfoxide
LD_{50}	light dose leading to 50% of cell death
MTT	3-[4,5-dimethylthiazol-2-yl]-2,5-diphenyl-tetrazolium bromide
ALA	aminolevulinic acid
Φ	efficiency of singlet oxygen formation
FBS	fetal bovine serum
PBS	phosphate buffer saline;
ECP	extracorporeal photopheresis.

INTRODUCTION

Photodynamic therapy (PDT) is a clinically validated treatment for superficial or accessible tumours [1–3]. The administration of a photosensitiser (PS) followed by irradiation with light induces PS excitation, and, in the presence of oxygen, produces reactive oxygen species that cause cytotoxicity in the tumour cells and vascularization leading to tumour damage [3]. In addition, PDT can stimulate immune responses [4].

PDT induces cell death through various mechanisms such as necrosis, apoptosis, paraptosis, autophagy, changes in the cell cycle and regulation of cell signalling pathways [5][6]. Photodamage usually involves the apoptotic pathways, though the use of PS at high doses can induce necrosis, which should be minimised because of the potential damage to surrounding cells [6]. PSs localised in the mitochondria usually provoke apoptosis very quickly, whereas those located in the lysosomes can evoke necrosis or apoptosis. In the plasma membrane, some targets for several PSs can induce both mechanisms of cell death [7].

The restricted number of clinically approved PSs is one of the factors hindering the progress of PDT [2,5]. On the other hand, World Health Organization strongly encourages the research in native medicinal plants in the search for potential new drugs [8,9]. In this regard, the study of new natural PSs is a promising area.

Although the first registered PSs were obtained from plants, synthetic PSs were the first to be approved for use in PDT, and thus natural PSs were overlooked [5]. In recent years, research has shifted from synthetic to natural chemotherapeutic drugs, due to their environmental sustainability and the low development of adverse effects. Many studies have even highlighted the use of herbal extracts for cancer treatment [10].

Anthraquinones (AQs) are the most abundant quinones in nature and can be found in plants, fungi, lichens and insects [11]. They are tricyclic organic compounds, with a great structural diversity, even among their synthetic derivatives, and therefore, they exhibit a diverse and interesting range of biological effects [12]. Furthermore, the structural features of AQs suggest their potential as PSs since they are flat, rigid molecules with a high degree of aromatic conjugation, and absorbs light of particular wavelengths [13,14]. Therefore, several AQ derivatives have been studied as possible PSs [15–17].

Our group has isolated several 9,10-anthraquinone aglycones from various natural sources, among which 1,8-dihydroxy-3-methoxy-6-methylanthraquinone, called parietin (PTN), is particularly attractive as PS. PTN is an orange dye that is found in several lichen families (Teloschistaceae, Brigantiaceae, Letroutiaceae, Psoraceae) and also in higher plants of the Rhamnus and Rheum families [18–21]. We have previously demonstrated the ability of PTN to act as a PS against bacteria mediated by the generation of superoxide anion and singlet oxygen after UVA-Vis illumination [22].

UVA-Vis light sources, such as actinic lamps (light range: 380–480 nm) that are generally employed in phototherapy of hyperbilirubinemia [23], are also used to excite AQs in PDT and Photodynamic antimicrobial chemotherapy [22,24–26]. It is well known that the light dose and the selection of the appropriate wavelength according to the absorption spectrum of the PS are critical factors that can improve the outcome of PDT [27].

In the present work, PTN was purified from the lichen *Teoloschistes nodulifer* (Nyl.) Hillman (Telochistaceae), and its photoactivity against tumour cells was evaluated, using UVA-Vis and blue light irradiation.

Since there is limited knowledge about the efficacy of blue light to photoinactivate eukaryotic cells treated with natural or synthetic AQs, we foresee putative applications of PTN and blue light in PDT.

MATERIALS AND METHODS

Chemicals

Deuterated chloroform ($CDCl_3$), MTT reagent (3-[4,5-dimethylthiazol-2-yl]-2,5-diphenyl-tetrazolium bromide), propidium iodide and RNAasa were obtained from Sigma Aldrich Corp (St. Louis, USA).

All other reagents and solvents were of analytical grade.

PTN extraction and purification

PTN (Figure 1) was extracted from the lichen *Teoloschistes nodulifer* (Nyl.) Hillman (Telochistaceae) collected in November 2015, in La Ventana, San Alberto department, Córdoba province, Argentina (GPS coordinates: 31° 31′ 46.3″ South latitude; 64° 51′ 51.0″ West longitude). It was identified by Dr C. Estrabou and J. M. Rodriguez (CERNAR, Facultad de Ciencias Físicas y Naturales, UNC, Argentina). A voucher specimen was deposited at the Museo Botánico de Córdoba (UNC) as CORDC00005354.

Dried and fragmented lichen (7.48 g) was exhaustively macerated with distilled acetone. The isolation of PTN (33.97 mg) from the dried extract was carried out by recrystallization in distilled ethyl acetate. Identification was performed by the analysis of their spectroscopic data (^{1}H-NMR, ^{13}C-NMR) in comparison with the data in the literature [28] (see

supplementary material). The purity of PTN was determined by HPLC-UV analysis by using a method previously described [26] (supplementary material).

PTN solution

Stock solutions of PTN (5 mM) in DMSO were kept at -70 ºC until its use. The solutions to be tested were prepared by diluting the stock with RPMI medium (Gibco, USA), which contained 5% fetal bovine serum (FBS, Natocor, Argentina) and a concentration of DMSO ≤ 1%.

Cell lines

Human myelogenous leukaemia K562 cells and IGROV-1 human ovarian cancer cells were obtained from the ATCC (Manassas, VA, USA).

LM2 murine mammary adenocarcinoma cells were kindly provided by Dr Ana M. Eiján from Instituto de Oncología Angel H. Roffo, Argentina [29]. HaCaT spontaneously immortalised human keratinocyte line was obtained from Dr. Quintanilla (Instituto de Investigaciones Biomédicas, Madrid, Spain). The cells were cultured in RPMI medium, supplemented with FBS (5% for LM2 and 10% for K562, HaCat and IGROV-1), 2 mM L-glutamine, 100 IU/ml penicillin, and 100 mg/ml streptomycin, at 37°C in a 5 % CO_2 atmosphere. K562 (1 x 10^5 cells/ml), LM2 (7 x 10^4 cells/ml), IGROV-1 (1 x 10^5 cells/ml) and HaCaT (6 x 10^4 cells/ml) cells were incubated in 24-well plates during 48 h.

Irradiation systems

Two irradiation systems were used: a) a UVA-Vis actinic lamp (Phillips TL 20 W/52, Germany) and b) an array consisting of 2 blue compact fluorescent lamps (Sica 15 W model 914173, Argentina). The emission spectrum of each light source was recorded on a Perkin Elmer LS55 fluorometer (Buckinghamshire, UK).

The cells were placed 14 cm above the light sources. The light fluences for the actinic and blue light systems were 0.65 mW/cm^2 and 4.7 mW/cm^2 respectively. The measurements were made with a Field Master power meter that has an LM3 HTP sensor (Coherent Inc., USA), which was placed at the position of the cells. At the end of the illumination, the cells

were incubated for 19 h to allow the generation of the photodamage, and then, the MTT viability assay was performed.

PTN uptake by K562 cells

K562 cells were exposed to different PTN concentrations (non-cytotoxic to cells) for 60 min at 37 °C. After 3 consecutive washes with phosphate buffer saline (PBS), the PTN accumulated inside the cells was extracted with DMSO for 30 min at 37 °C, and the fluorescence was recorded in a Perkin Elmer LS55 fluorometer (Buckinghamshire, UK) employing λ_{exc}= 432 nm and λ_{em}= 591 nm. Intracellular PTN was quantified by extrapolation on a calibration curve (fluorescence *vs* PTN concentration) made from dilutions of the PTN standard solutions in DMSO and expressed per cell number.

Transport mechanism of PTN into K562 cells

The contribution of passive diffusion to PTN transport in K562 cells was determined: i) exposing the cells to cold PTN in complete medium and afterwards incubating for 60 min at 4°C or ii) exposing the cells to pre-warmed PTN in full medium and incubating at 37°C for 60 min. After two washings with cold PBS, a PTN-PDT treatment was performed to infer the proportion of PTN incorporated by the degree of photodamage.

PTN-PDT treatment

K562, LM2, IGROV-1 and HaCaT cells were seeded in 24-well plates for 2 days before exposure to PTN. After the addition of PTN (complete medium), they were incubated at different times: 1 h for PTN at 30 μM and 24 h for PTN at 3 μM . PTN was then replaced with fresh medium and irradiations were performed. After irradiation, the cells were incubated during 19 h and finally, cell viability was tested. The light doses (LD_{50}, LD_{75}, and LD_{95}) leading to 50%, 75% and 95% cell death were calculated in J/cm^2. No changes in the temperature of the cell media were recorded during illumination with both light sources.

Cell cycle analysis after PTN-PDT

K562 cells (1 x 10^5 cells/ml) were seeded in 6-well plates two days before PTN treatment. Once PTN was added, it was incubated for 1 h (30 μM) or 24 h (3 μM). The PTN solution

was then replaced with fresh medium, and the cells were irradiated with the blue lamp at different light doses. The method described by Crissman was used to evaluate the different cell cycle populations [30]. The method involves treating cells with propidium iodide, which binds to DNA by intercalating between bases, and allows the cell DNA content to be quantified at different phases. These measurements are used to differentiate cells at G_1-, S- and G_2/M phase, and Sub-G1 (apoptotic cells). Propidium iodide emits a fluorescent signal when is excited at 488 nm with a broad emission centred around 600 nm.

The cells were incubated for further 19 h, after that, they were fixed with 70% ethanol at -20 °C for 30 min. Subsequently, the cells were treated with RNAase and incubated with propidium iodide before the analysis. Cell cycle distribution was evaluated using a BD FACSCalibur flow cytometer (BD Biosciences, Jan Jose, CA, USA). Data analysis was performed employing FlowJo 10.0.7 software 2.8. In parallel experiments, the toxicity was checked by means of the MTT viability test.

MTT viability assay

The MTT assay [31] was used to determine cell death after PTN-PDT and PTN dark toxicity [30]. The absorbance of the resulting formazan was quantified at 560 nm in an Epoch microplate reader (BioTek, USA).

Statistical analysis

All assays were evaluated in triplicates in 3 independent experiments. Data were expressed as means with standard deviations. The data were analysed statistically by using the computational statistical software Origin 8.5. Student's t-Test and two-way ANOVA with a value of $p < 0.05$ were used to consider a statistically significant difference. The values of LD_{50}, LD_{75} and LD_{95} were obtained from the dose-response curves, with non-linear regression analysis (Sigmoidal Origin, $R^2 > 0.9$).

RESULTS

Emission spectra of lamps and absorbance spectrum of PTN

We analysed the emission spectra of the actinic and blue lamp used in the PTN excitation (Figure 2). The actinic lamp exhibited a wide and prominent emission peak in the 380-

480 nm range, and two minor peaks in the green (546 nm) and yellow (578 nm) areas of the spectrum. On the other hand, the blue light shows a wide emission area in the 395-525 nm range of visible light.

PTN showed a pronounced absorption peak in the UV together with a wide absorption area in the visible light region with maxima at 437 nm and a shoulder at 515 nm. Therefore, the blue light array covers all the visible light absorption range of PTN.

Light-induced cytotoxicity

To define the maximum dose of light that could be applied to K562 cells, we defined 20% cell death as the admitted limit (Figure 3). Therefore, 1.4 J/cm^2 and 25.5 J/cm^2 were the maximum desirable doses of UVA-Vis and blue light, respectively. The lower toxicity induced by blue light compared to UVA-Vis, together with the analysis of the spectra, led us to choose the blue light system to carry out the photosensitisation experiments.

PTN cellular uptake

Although PTN (purity=95.5 ± 0.2%) did not exhibit significant toxicity at the tested concentrations (0 to 50 µM) with 24 h of incubation, it formed microscopically visible crystals at doses higher than 30 µM (1% DMSO as co-solvent). Therefore, the maximum dose used was 30 µM (see supplementary material). The amount of PTN taken up by the cells was linear in the range of PTN added to the cells (1 to 30 µM), suggesting the involvement of passive diffusion in the transport of the PS into the cells (Figure 4).

Mechanism of cellular uptake of PTN

Figure 5 shows the contribution of passive transport of PTN, inferred from its differential photodynamic effect at 4 °C and 37 °C. An active transport system would be completely blocked by lowering the temperature to 4 °C, whereas the participation of passive transport would be suggested in the uptake of the PS at this low temperature [32].

The figure shows that even when PTN uptake was carried out at 4°C, the response of the cells to PDT was markedly high and was only lowered by 30% compared to the uptake at 37°C. Since membrane fluidity is higher when the temperature is increased, the response at 37°C is expected to be higher. Therefore, the data suggest that there is no involvement of a

specific energy-dependent drug incorporation pathway, and passive diffusion is the primary mechanism involved in PTN incorporation into K562 cells.

PTN-mediated PDT

The light dose-response curve of PTN-PDT was carried out at *a*) low PTN concentration (3 μM) and long exposure times (24 h) or *b*) high PTN concentration (30 μM) and short exposure periods (1 h). LD_{50}s obtained were 8 J/cm^2 and 2.1 J/cm^2 for protocols *a* and *b*, respectively (Figure 6).

Cell cycle analysis after PTN-PDT

The effect of PTN-PDT treatment on the cell cycle was evaluated by flow cytometry on K562 cells (Figure 7). The two protocols described above were performed: *a*) 3 μM PTN 24 h exposure and *b*) 30 μM PTN 1 h exposure, applying light doses corresponding to LD_{50}, LD_{75} and LD_{95} for each condition.

Cell cycle analysis shows that the percentage of Sub-G1 (apoptotic) cells increased with PDT-PTN treatment. The percentage of Sub-G1 events increased significantly in cells treated with PTN-PDT: 2.7% control vs 20% and 13% in PTN-PDT treated with LD_{50} and LD_{75} respectively in Protocol *a*, and 3.7% control vs 20% and 15% in PTN-PDT treated with LD_{50} and LD_{75} respectively in Protocol *b*. Moreover, whereas LD_{50} and LD_{75} induced similar percentages of Sub G1 events, in cells treated with LD_{95} these percentages were even more marked (55% for Protocol *a* and 37% for Protocol *b*).

PTN-PDT in a small panel of cell lines

After finding the optimal conditions for PTN-PDT treatment that induce photokilling of K562 cells, the outcome of the treatment was evaluated by illuminating with blue light two additional tumour cell lines: murine adenocarcinoma LM2 cells and human ovarian cancer IGROV-1 cells, and also in a normal HaCaT human keratinocytes (Figure 8).

All four cell lines tested were effectively photosensitised by the treatment. Besides, IGROV-1 was the cell line most resistant to PTN-PDT, HaCaT the most sensitive ($p < 0.01$, two-way ANOVA) and LM2 and K562 cells were equally sensitive to the treatment.

Discussion

In previous work, PTN induced the production of superoxide radical anion in human neutrophils after UVA-Vis illumination. Besides, PTN inactivated *Staphylococcus aureus*, *Staphylococcus epidermidis* and *Pseudomonas aeruginosa* after excitation with the same light source [22]. Even other AQs, such as rubiadin and rubiadin 1-methyl ether, photoinactivated *Candida tropicalis* biofilms under UVA-Vis illumination [34]. However, the UVA-Vis light source employed in this work, induced considerable toxicity in K562 cells, whereas blue light exerted a low toxicity, even at high doses

PTN has a major absorption peak in the UVA region, and a second peak in the blue-violet wavelengths [33]. It is well known that blue light is much less harmful to eukaryotic cells than UV irradiation [34][35] and, furthermore, UV light barely penetrates at all and blue light barely penetrates 1 mm into the skin [35].

For antimicrobial photoinactivation, it has been reported that the most efficient wavelength range is violet (~390 to 420 nm), and the next most effective is blue light (450 to 480 nm) [36]. However, the longer excitation wavelengths penetrate deeper into the tissues and are desired for effective cancer treatment [37]. Blue light has been used successfully in the treatment of skin cancers such as basal cell carcinomas [38] and melanomas [39]. Differences in the depth of light penetration are due to the chromophores present in the skin, which have scattering and absorption coefficients that are very dependent on wavelength [37].

Actinic keratoses, which are premalignant skin lesions based on the hyperproliferation of keratinocytes, are usually treated with PDT. Therefore, it is important that we found that keratinocytes can be effectively photodamaged by the use of PTN and blue light.

In the present work, we also showed that light doses of approximately 8 J/cm^2 almost completely eradicated cells of different origins such as mammary tumour (LM2), leukaemic (K562) and keratinocytes (HaCaT) employing 30 µM PTN. In addition, doses between 1.4 and 3 J/cm^2 were needed to photoinactivate 50% of these cells, and also of ovary adenocarcinoma IGROV-1.

Other natural AQs such as soranjididol, 5-chloro soranjidiol, bisoranjidiol, 7-chloro bisoranjidiol and lycionine, induced photokilling of fibroblasts with violet-blue LEDs ($\lambda = 410 \pm 10$ nm) employing fluences of 27 J/cm^2, that is, a light dose notably higher than that required in the present work [40].

Light doses of 6 to 12 J/cm^2 emitted by a 405 nm diode laser photokilled 50 to 75% of the KB epidermal carcinoma cells employing other natural AQs such as aloe emodin, which exhibits moderate absorption of blue light [41].

Extracorporeal photopheresis (ECP), an accepted modality for cutaneous T-cell lymphoma, involves the *ex vivo* illumination of leukocytes with UVA light after exposure to 8-methoxypsoralen and subsequent reinfusion into the patient [42]. PDT mediated by 5-aminolevulinic acid (ALA) and UV illumination has been proposed as an alternative treatment to ECP [43]. Besides, *ex vivo* ALA-PDT has been useful in the removal of residual leukaemic cells in the transplantation of auto-hematopoietic stem cells after high-dose chemotherapy in T-cell leukaemias or lymphomas [44][45]**.** In such procedures, buffy coat - that is leukocytes and platelets- is exposed to PS and light, thus avoiding interference of light absorption by haemoglobin. In addition, PDT mediated by PSs such as merocyanine 540 [46] and Victoria blue BO was useful and selective against leukaemic cells [45] [47].

In the present work, we were able to efficiently photosensitise leukaemic cells of myeloid origin by employing a natural PS and visible light, which is an interesting alternative to the use of ECP and elimination of leukaemic cells in the transplantation of auto-hematopoietic stem cells.

Passive transport appears to be the main mechanism involved in the entry of PTN into the cells. The linearity of PTN uptake as a function of concentrations, together with the lack of influence of temperature on the process, support the hypothesis of passive uptake. AQ aglycons show a log P between 1.2 to 2.8 [48], which makes them capable of being taken up by cells without a transport-mediated mechanism [49]. Moreover, doxorubicin AQ is a powerful and widely used antineoplastic that is transported by passive diffusion [50].

Apoptosis, together with necrosis, paraptosis, and autophagy are the mechanisms implicated in photodynamic cell killing [6]**.** Apoptotic cell death is usually correlated with low light-dose, as low ROS levels are presumed to induce a cell-signalling cascade that leads to apoptotic cell death [5]. At high light-dose, conformational change in lipids can

induce phase separation of the plasma membrane [51], promoting breakdown and thus leading to necrotic cell death or lysis [52]. Furthemore, it has been proposed that the wavelength of the light can affect the mechanism of cell death. Hexyl-ALA-PDT with red light, provoked more apoptosis than the same procedure with blue light, and in addition, PDT with low irradiance induced a higher degree of apoptotic cell death compared to high irradiance employing equal doses of lethal light [53].

To study the influence of light dose and the exposure to PS on the outcome of PDT, and the mechanism of cell death, we applied two protocols: *a*) exposure at 3 µM PTN for 24 h and *b*) 30 µM PTN for 1 h. In both protocols, a considerably high percentage of sub-G1 cells (presumably apoptotic) [54] was reached, and the percentage of sub-G1 events was markedly higher when the highest light dose was employed.

Other authors demosntrated that PTN was significantly cytotoxic in the dark when it was used at concentrations from 50 µM onwards after 72 h exposure, with a low percentage of apoptotic cells [53]. In addition, PDT mediated by other natural AQs such as rubiadin and soranjidiol produced apoptosis involving the caspases-3-independent pathway after UVA-Vis irradiation with 1 J/cm^2 [25].

The yield of singlet oxygen generation (Φ) of AQ derivatives depends on the nature and position of the substituents [55]. This PTN parameter in chloroform was calculated in previous studies to be 0.69 [25], which is higher compared to other natural AQs such as soranjidiol (Φ = 0.47) and rubiadin (Φ = 0.34) and only lower than nordamcanthal (Φ = 0.84) [56].

Therefore, due to its high singlet oxygen quantum yield, efficient uptake by cells and the lower irradiance required to exert its photosensitising effect compared to related compounds, PTN is a promising PS using blue light illumination. This feature makes it appropriate for the treatment of superficial malignancies or as an aid in purging leukaemic cells. Furthermore, the replacement of traditional light sources containing UV-light by visible blue light that significantly photoactivates AQs was achieved. These findings are encouraging in the field of photodynamic killing of eukaryotic cells mediated by AQs. Further *in vivo* studies will be needed to assess the PTN selectivity for tumour cells.

Conflicts of interest

The authors declare that they have no conflict of interest.

Acknowledgements

MLM, GC, JM and FM are research fellow of CONICET, MC. AC, JLC, SCNM, GDV, and DS are members of the Research Career of CONICET, Argentina. AC thanks to ANPCyT (PICT 2014-0727) and CONICET (PIP 2014 number 11220130100237CO). SCNM is grateful for the financial support of the Argentinian agencies SeCyT-UNC 2016-2017, Proyecto Consolidar 2018-2020, and ANPCyT (PICT 2014-2204 and PICT 2016-1697).

Credit author statement:

MLM: Investigation, Methodology, Analysis; Manuscript writing **GC:** Methodology; Analysis; **JM**: Methodology; **MC**: Methodology; **FM**: Methodology; **DS**: Methodology, Supervision; **GDV:** Methodology, Supervision; **JLC**: Supervision; **SNM**: Review & editing, Funding acquisition; **AC:** Conceptualization, Funding acquisition, writing- original draft.

Declaration of interest: None

References

[1] R. Bonnett, Photosensitisers of the porphyrin and phthalocyanine series for photodynamic therapy, Chem. Soc. Rev. 24 (1995) 19. https://doi.org/10.1039/cs9952400019.

[2] M.R. Hamblin, Photodynamic Therapy for Cancer: What's Past is Prologue, Photochem. Photobiol. (2019). https://doi.org/10.1111/php.13190.

[3] P. Acedo, J.C. Stockert, M. Cañete, A. Villanueva, Two combined photosensitisers: A goal for more effective photodynamic therapy of cancer, Cell Death Dis. 5 (2014) 1–12. https://doi.org/10.1038/cddis.2014.77.

[4] A.P. Castano, P. Mroz, M.R. Hamblin, Photodynamic therapy and anti-tumour immunity, Nat. Rev. Cancer. (2006). https://doi.org/10.1038/nrc1894.

[5] B. Siewert, H. Stuppner, The photoactivity of natural products – An overlooked potential of phytomedicines?, Phytomedicine. 60 (2019) 152985. https://doi.org/10.1016/j.phymed.2019.152985.

[6] D. Kessel, Apoptosis, Paraptosis and Autophagy: Death and Survival Pathways

Associated with Photodynamic Therapy, Photochem. Photobiol. (2019). https://doi.org/10.1111/php.12952.

[7] A.C.E. Moor, Signaling pathways in cell death and survival after photodynamic therapy, J. Photochem. Photobiol. B Biol. (2000). https://doi.org/10.1016/S1011-1344(00)00065-8.

[8] F.W. Health, A. Geneva, WHA41.19 Traditional medicine and medicinal plants, II (2000) 1988.

[9] World Health Organization (WHO), WHO Policy System Traditional medicine, Geneva World Heal. Organ. II (1987) 1987.

[10] P.P. Fu, H.M. Chiang, Q. Xia, T. Chen, B.H. Chen, J.J. Yin, K.C. Wen, G. Lin, H. Yu, Quality assurance and safety of herbal dietary supplements, J. Environ. Sci. Heal. - Part C Environ. Carcinog. Ecotoxicol. Rev. 27 (2009) 91–119. https://doi.org/10.1080/10590500902885676.

[11] H. Dave, L. Ledwani, A review on anthraquinones isolated from Cassia species and their applications, Indian J. Nat. Prod. Resour. 3 (2012) 291–319.

[12] J. Deitersen, D.H. El-Kashef, P. Proksch, B. Stork, Anthraquinones and autophagy – Three rings to rule them all?, Bioorganic Med. Chem. 27 (2019) 115042. https://doi.org/10.1016/j.bmc.2019.115042.

[13] L.M. Baltazar, A. Ray, D.A. Santos, P.S. Cisalpino, A.J. Friedman, J.D. Nosanchuk, Antimicrobial photodynamic therapy: An effective alternative approach to control fungal infections, Front. Microbiol. (2015). https://doi.org/10.3389/fmicb.2015.00202.

[14] M.R. Hamblin, Antimicrobial photodynamic inactivation: a bright new technique to kill resistant microbes, Curr. Opin. Microbiol. (2016). https://doi.org/10.1016/j.mib.2016.06.008.

[15] G. Pfaffel-Schubart, A. Rück, C. Scalfi-Happ, Modulation of cellular Ca2+-signaling during hypericin-induced photodynamic therapy (PDT), Med. Laser Appl. 21 (2006) 61–66. https://doi.org/10.1016/j.mla.2005.12.001.

[16] M. Waser, H. Falk, Towards Second Generation Hypericin Based Photosensitisers for Photodynamic Therapy, Curr. Org. Chem. 11 (2007) 547–558. https://doi.org/10.2174/138527207780368229.

[17] X. Schneider-Yin, A. Kurmanaviciene, M. Roth, M. Roos, A. Fedier, E.I. Minder, H. Walt, Hypericin and 5-aminolevulinic acid-induced protoporphyrin IX induce enhanced phototoxicity in human endometrial cancer cells with non-coherent white light, Photodiagnosis Photodyn. Ther. 6 (2009) 12–18. https://doi.org/10.1016/j.pdpdt.2009.02.001.

[18] E. Lopez-Tobar, V. Verebova, L. Blascakova, D. Jancura, G. Fabriciova, S. Sanchez-Cortes, Detection and aggregation of the antitumoral drug parietin in ethanol/water mixture and on plasmonic metal nanoparticles studied by surface-enhanced optical spectroscopy: Effect of pH and ethanol concentration, Spectrochim. Acta - Part A Mol. Biomol. Spectrosc. 159 (2016) 134–140. https://doi.org/10.1016/j.saa.2016.01.033.

[19] J. Hafellner, A world monograph of Brigantiaea (lichenised Ascomycotina, Lecanorales) The Alps-a global reference area for lichen diversity in high mountains View project, n.d. https://www.researchgate.net/publication/309210626 (accessed May 15, 2020).

[20] S. Johansson, U. Søchting, J.A. Elix, J.H. Wardlaw, Chemical variation in the lichen genus Letrouitia (Ascomycota, Letrouitiaceae), Mycol. Prog. (2005). https://doi.org/10.1007/s11557-006-0117-5.

[21] K.A. Solhaug, Y. Gauslaa, Parietin, a photoprotective secondary product of the lichen Xanthoria parietina, Oecologia. (1996). https://doi.org/10.1007/BF00333715.

[22] L.R. Comini, F.F. Morán Vieyra, R.A. Mignone, P.L. Páez, M. Laura Mugas, B.S. Konigheim, J.L. Cabrera, S.C. Núñez Montoya, C.D. Borsarelli, Parietin: an efficient photo-screening pigment in vivo with good photosensitising and photodynamic antibacterial effects in vitro, Photochem. Photobiol. Sci. (2017). https://doi.org/10.1039/C6PP00334F.

[23] Phototherapy lamps | Philips lighting, (n.d.). https://www.lighting.philips.com/main/products/special-lighting/phototherapy (accessed May 23, 2020).

[24] L.R. Comini, I.M. Fernandez, N.B.R. Vittar, S.C. Núñez Montoya, J.L. Cabrera, V.A. Rivarola, Photodynamic activity of anthraquinones isolated from Heterophyllaea pustulata Hook f. (Rubiaceae) on MCF-7c3 breast cancer cells,

Phytomedicine. (2011). https://doi.org/10.1016/j.phymed.2011.05.008.

[25] N.B. Rumie Vittar, L. Comini, I.M. Fernadez, E. Agostini, S. Nuñez-Montoya, J.L. Cabrera, V.A. Rivarola, Photochemotherapy using natural anthraquinones: Rubiadin and Soranjidiol sensitize human cancer cell to die by apoptosis, Photodiagnosis Photodyn. Ther. (2014). https://doi.org/10.1016/j.pdpdt.2014.02.002.

[26] J. Marioni, M.A. da Silva, J.L. Cabrera, S.C.N. Montoya, M.G. Paraje, The anthraquinones rubiadin and its 1-methyl ether isolated from Heterophyllaea pustulata reduces Candida tropicalis biofilms formation, Phytomedicine. (2016). https://doi.org/10.1016/j.phymed.2016.07.008.

[27] H. Abrahamse, I. Sosthene Mfouo Tynga, Photodynamic Therapy, a Potential Therapy for Improve Cancer Management, Breast Cancer Surg. (2018). https://doi.org/10.5772/intechopen.74697.

[28] Aislamiento de ácido úsnico y parietina de Caloplaca saxicola Hoffm., Rev. ECIPeru. (2019). https://doi.org/10.33017/reveciperu2011.0016/.

[29] S. Galli, L. Colombo, S. Vanzuli, M.C. Daroqui, M. del Carmen Vidal, M.A. Jasnis, E. Sacerdote de Lustig, A.M. Eijan, Characterisation of a fibroblastoid mammary carcinoma cell line (LM2) originated from a mouse adenocarcinoma., Int. J. Oncol. (2000). https://doi.org/10.3892/ijo.17.6.1259.

[30] H.A. Crissman, J.A. Steinkamp, Rapid, simultaneous measurement of DNA, protein, and cell volume in single cells from large mammalian cell populations, J. Cell Biol. (1973). https://doi.org/10.1083/jcb.59.3.766.

[31] F. Denizot, R. Lang, Rapid colorimetric assay for cell growth and survival. Modifications to the tetrazolium dye procedure giving improved sensitivity and reliability, J. Immunol. Methods. (1986). https://doi.org/10.1016/0022-1759(86)90368-6.

[32] A. Smith, W.T. Morgan, Hemopexin-mediated transport of heme into isolated rat hepatocytes., J. Biol. Chem. 256 (1981) 10902–109.

[33] S. Huneck, I. Yoshimura, Identification of Lichen Substances, 1996. https://doi.org/10.1007/978-3-642-85243-5.

[34] J. Liebmann, M. Born, V. Kolb-Bachofen, Blue-light irradiation regulates proliferation and differentiation in human skin cells, J. Invest. Dermatol. (2010).

https://doi.org/10.1038/jid.2009.194.

[35] M.M. Kleinpenning, T. Smits, M.H.A. Frunt, P.E.J. van Erp, P.C.M. van de Kerkhof, R.M.J.P. Gerritsen, Clinical and histological effects of blue light on normal skin, Photodermatol. Photoimmunol. Photomed. (2010). https://doi.org/10.1111/j.1600-0781.2009.00474.x.

[36] M.R. Hamblin, H. Abrahamse, Can light-based approaches overcome antimicrobial resistance?, Drug Dev. Res. (2019). https://doi.org/10.1002/ddr.21453.

[37] C. Ash, M. Dubec, K. Donne, T. Bashford, Effect of wavelength and beam width on penetration in light-tissue interaction using computational methods, Lasers Med. Sci. (2017). https://doi.org/10.1007/s10103-017-2317-4.

[38] E. V. Maytin, U. Kaw, M. Ilyas, J.A. Mack, B. Hu, Blue light versus red light for photodynamic therapy of basal cell carcinoma in patients with Gorlin syndrome: A bilaterally controlled comparison study, Photodiagnosis Photodyn. Ther. (2018). https://doi.org/10.1016/j.pdpdt.2018.02.009.

[39] R.A. Akasov, N. V. Sholina, D.A. Khochenkov, A. V. Alova, P. V. Gorelkin, A.S. Erofeev, A.N. Generalova, E. V. Khaydukov, Photodynamic therapy of melanoma by blue-light photoactivation of flavin mononucleotide, Sci. Rep. (2019). https://doi.org/10.1038/s41598-019-46115-w.

[40] J.A. Dimmer, C. Ramos Silva, S.C. Nunez Montoya, J.L. Cabrera, M.S. Ribeiro, Photodynamic activity of natural anthraquinones on fibroblasts, in: 2018. https://doi.org/10.1117/12.2290666.

[41] L. Zang, H. Zhao, X. Ji, W. Cao, Z. Zhang, P. Meng, Photophysical properties, singlet oxygen generation efficiency and cytotoxic effects of aloe emodin as a blue light photosensitiser for photodynamic therapy in dermatological treatment, Photochem. Photobiol. Sci. (2017). https://doi.org/10.1039/c6pp00453a.

[42] R. Edelson, C. Berger, F. Gasparro, B. Jegasothy, P. Heald, B. Wintroub, E. Vonderheid, R. Knobler, K. Wolff, G. Plewig, G. McKiernan, I. Christiansen, M. Oster, H. Honigsmann, H. Wilford, E. Kokoschka, T. Rehle, M. Perez, G. Stingl, L. Laroche, Treatment of Cutaneous T-Cell Lymphoma by Extracorporeal Photochemotherapy, N. Engl. J. Med. (1987). https://doi.org/10.1056/NEJM198702053160603.

[43] T. Holien, O.A. Gederaas, S.R. Darvekar, E. Christensen, Q. Peng, Comparison between 8-methoxypsoralen and 5-aminolevulinic acid in killing T cells of photopheresis patients ex vivo, Lasers Surg. Med. (2018). https://doi.org/10.1002/lsm.22806.

[44] Z. Hrkal, D. Grebenová, H. Cajthamlová, J. Soucek, J. Bartosová, O. Fuchs, I. Marinov, P. Kobylka, H. Klamová, D. Sponerová, Use of photodynamic therapy for elimination of residual leukemic cells in autologous transplants of hematopoietic progenitor cells, Cas. Lek. Cesk. (2002).

[45] B. Underlíková, V. Vasovi, F. Sieber, T. Furre, E. Borgen, J.M. Nesland, Q. Peng, Hexaminolevulinate-mediated photodynamic purging of marrow grafts with murine breast carcinoma, Bone Marrow Transplant. (2011). https://doi.org/10.1038/bmt.2010.277.

[46] K.S. Gulliya, J.W. Fay, R.M. Dowben, S. Berkenkilder, J.L. Matthews, Elimination of leukemic cells by laser photodynamic therapy, Cancer Chemother. Pharmacol. (1988). https://doi.org/10.1007/BF00273413.

[47] M. Fiedorowicz, A. Pituch-Nowor olska, M. Zembala, The photodynamic effect of Victoria blue BO on peripheral blood mononuclear and leukemic cells, Photochem. Photobiol. (1997). https://doi.org/10.1111/j.1751-1097.1997.tb01934.x.

[48] L.R. Comini, S.C. Núñez Montoya, G.A. Argüello, J.L. Cabrera, Determinación del coeficiente de partición (log P) para derivados antraquinónicos aislados de Heterophyllaea pustulata Hook. f. (Rubiáceas), Acta Farm. Bonaer. (2006).

[49] J.C. Stockert, A. Juarranz, A. Villanueva, S. Nonell, R. Horobin, A. Soltermann, E.N. Durantini, V. Rivarola, L. Colombo, J. Espada, M. Cañete, Photodynamic therapy: Selective uptake of photosensitising drugs into tumor cells, Curr. Top. Pharmacol. 8 (2014) 185–217.

[50] G. Speelmans, R.W.H.M. Staffhorst, F.A. De Wolf, B. De Kruijff, Verapamil competes with doxorubicin for binding to anionic phospholipids resulting in increased internal concentrations and rates of passive transport of doxorubicin, BBA - Biomembr. (1995). https://doi.org/10.1016/0005-2736(95)00119-N.

[51] C. Gajate, F. Gonzalez-Camacho, F. Mollinedo, Lipid raft connection between extrinsic and intrinsic apoptotic pathways, Biochem. Biophys. Res. Commun.

(2009). https://doi.org/10.1016/j.bbrc.2009.01.147.

[52] A.P. Castano, T.N. Demidova, M.R. Hamblin, Mechanisms in photodynamic therapy: Part one - Photosensitisers, photochemistry and cellular localisation, Photodiagnosis Photodyn. Ther. (2004). https://doi.org/10.1016/S1572-1000(05)00007-4.

[53] L. Helander, H.E. Krokan, A. Johnsson, O.A. Gederaas, K. Plaetzer, Red versus blue light illumination in hexyl 5-aminolevulinate photodynamic therapy: the influence of light color and irradiance on the treatment outcome in vitro , J. Biomed. Opt. (2014). https://doi.org/10.1117/1.jbo.19.8.088002.

[54] D. Plesca, S. Mazumder, A. Almasan, Chapter 6 DNA Damage Response and Apoptosis, Methods Enzymol. (2008). https://doi.org/10.1016/S0076-6879(08)01606-6.

[55] I.M. Byteva, G.P. Gurinovich, O.L. Golomb, V. V. Karpov, Anthraquinone derivatives as sensitisers of the formation of singlet oxygen, J. Appl. Spectrosc. (1986). https://doi.org/10.1007/BF00661049.

[56] L. Comini, S. Núñez Montoya, G. Argüello, J. Cabrera, Photophysical, photochemical and photobiological properties of anthraquinones isolated from a phototoxic vegetal species: Heterophyllaea pustulata, 12 (2010).

Figure 1: Structure of parietin (1,8-dihydroxy-3-methoxy-6-methyl-9,10-anthraquinone)

Figure 2: Emission spectrum of lamps and absorbance spectrum of parietin in DMSO

Figure 3: Response of K562 cells to different light doses applied by two irradiation systems

Cells were irradiated with different light doses employing an actinic (UVA-Vis) lamp and a blue lamp array. MTT was performed to evaluate cell viability and the results were expressed as the percentage of the non-illuminated controls *$p < 0.05$ as compared to the non-illuminated controls (*t*-Test).

Figure 4: Cellular uptake of PTN as a function of the concentration

K562 cells were exposed to different concentrations of PTN during 1 h at 37 °C. Intracellular PTN levels were quantified and expressed per cell number.

Figure 5: Mechanism of PTN transport into K562 cells

Cells were exposed to 30 µM PTN at 4°C or 37°C during 1 h and afterwards, PDT was carried out employing illumination with 2 J/cm^2 of blue light. Cell survival to PTN-PDT was determined as an indirect indicator of the PTN incorporation into the cells. Controls of non-treated cells and PTN-treated non-illuminated cells were included. *p<0.001, 37 °C as compared to 4 °C (*t*-Test).

Figure 6: K562 cell response to PTN-PDT at different blue light doses employing two protocols

K562 cells were PTN-PDT treated under 2 protocols: *a*) 3 µM PTN 24 h exposure and *b*) 30 µM PTN 1 h exposure, applying different blue light doses. Cell viability was expressed as the percentage of the non-illuminated controls.

Figure 7: Cell cycle distribution of K562 cells exposed to PTN-PDT

K562 cells were exposed 24 h to 3 µM PTN (Protocol *a*) and irradiated with 2.1 J/cm^2, 3 J/cm^2 or 8.5 J/cm^2, or exposed 1 h to 30 µM PTN and irradiated with 8 J/cm^2, 12.4 J/cm^2 or 25.6 J/cm^2 (Protocol *b*), which corresponds to LD_{50}, LD_{75} or LD_{95} respectively. Cell cycle was analysed after 19 h of photodamage by flow cytometry after propidium iodide staining. Controls of PTN-treated or illuminated with LD_{95} were included. A representative DNA histogram of each condition (A) and cell cycle analysis (B) are shown.

Figure 8: Response to PTN-PDT in a panel of cell lines

Cells were incubated 1 h with PTN at 30 µM and illuminated with different doses of blue light. Cell viability was evaluated and expressed as the percentage of the non-illuminated controls. LD_{50}s have been calculated.

Graphical abstract:

Highlights:

- The natural anthraquinone parietin photosensitises leukaemic cells.
- Blue light induces efficient parietin excitation.
- PDT employing parietin induces apoptosis of leukaemic cells.
- Ovary and mammary cancer cells and keratinocytes, respond also to PTN-PDT.

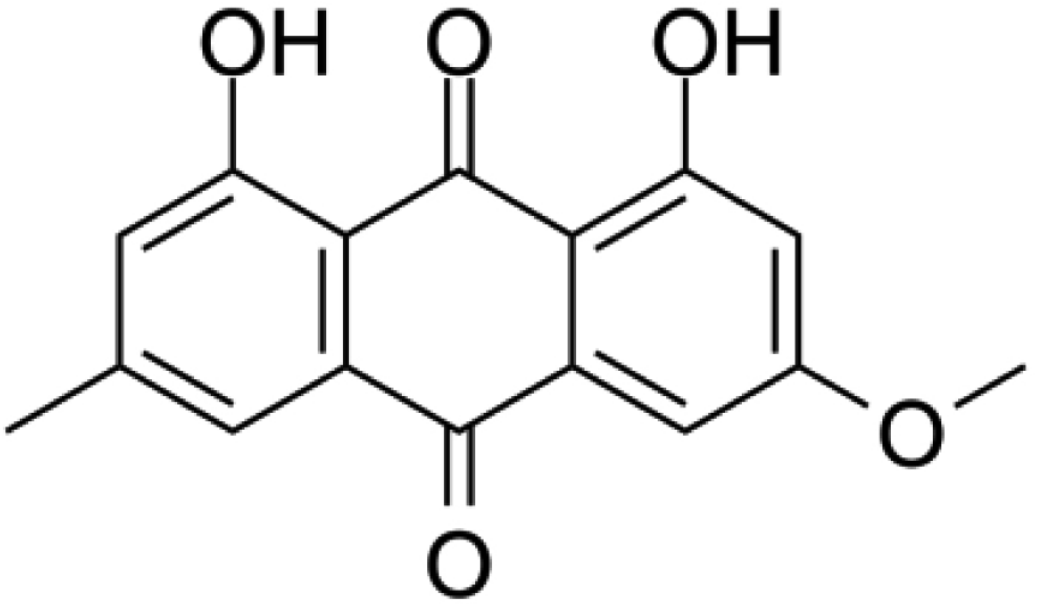

Figure 1

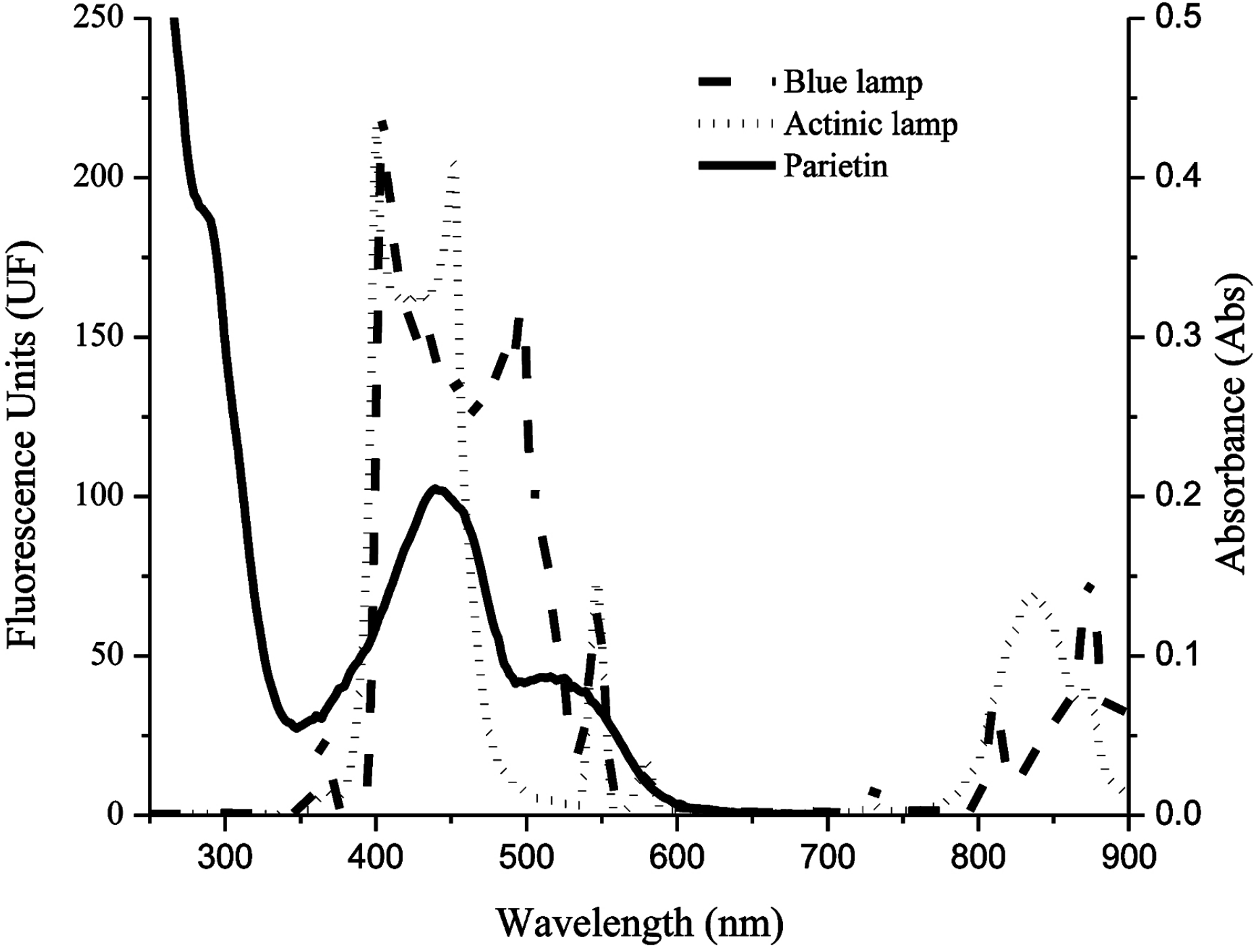
Blue lamp
Actinic lamp
Parietin
Fluorescence Units (UF)
Absorbance (Abs)
Wavelength (nm)
250
200
150
100
50
0
0.5
0.4
0.3
0.2
0.1
0.0
300
400
500
600
700
800
900

Figure 2

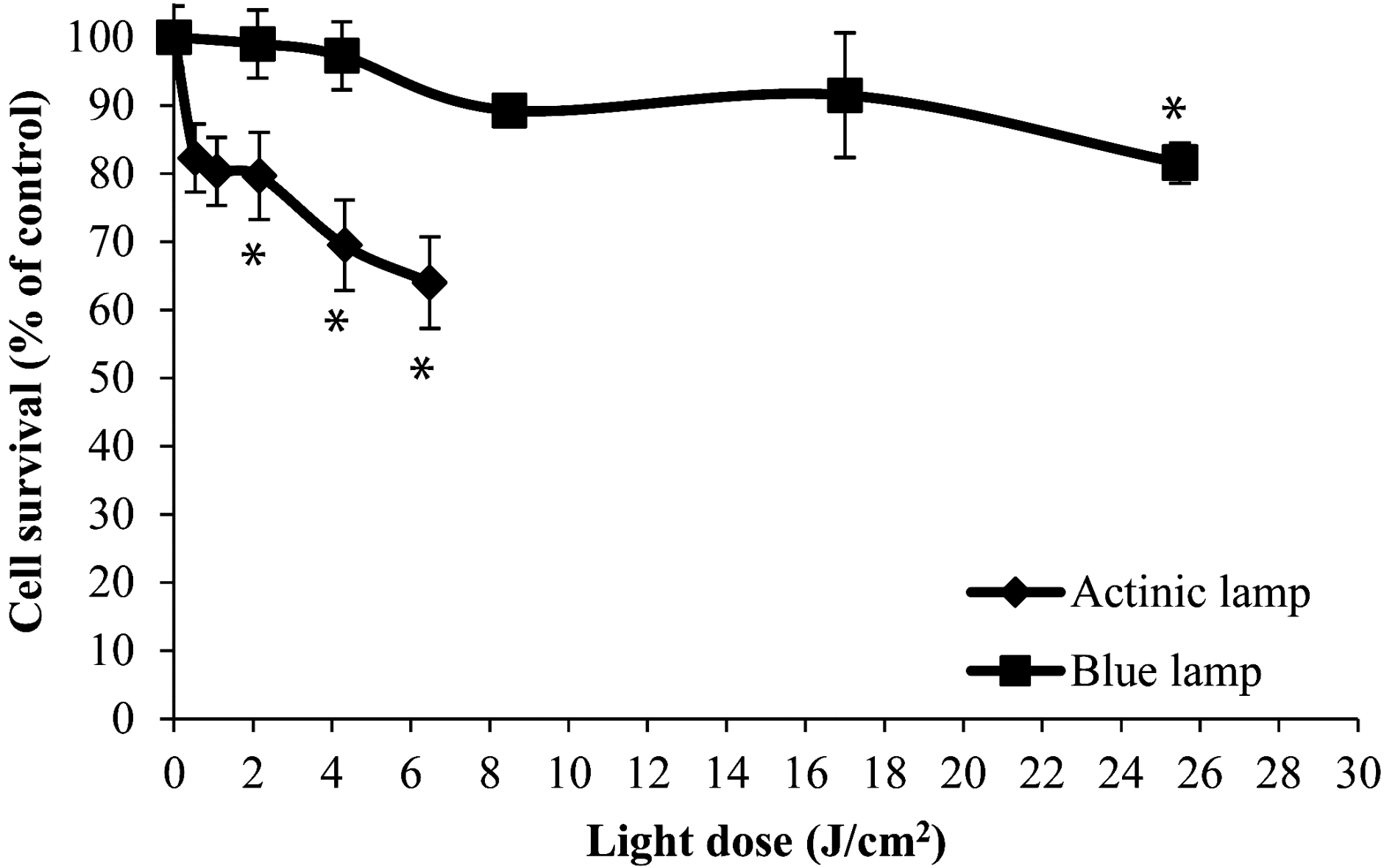
Cell survival (% of control)
100
90
80
70
60
50
40
30
20
10
0
0
2
4
6
8
10
12
14
16
18
20
22
24
26
28
30
Light dose (J/cm²)
Actinic lamp
Blue lamp
*
*
*
*

Figure 3

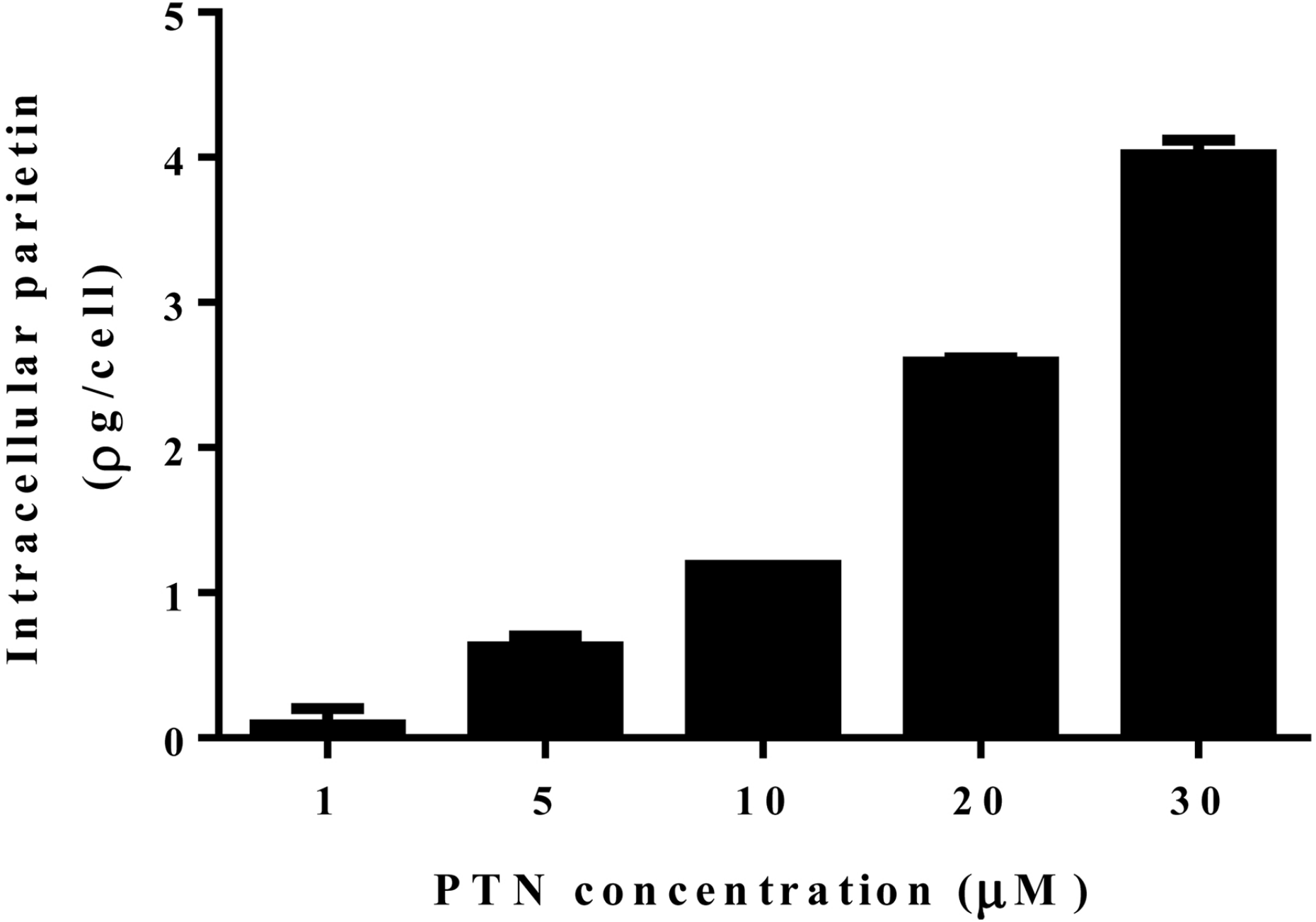
Intracellular parietin (ρg/cell)
5
4
3
2
1
0
1
5
10
20
30
PTN concentration (μM)

Figure 4

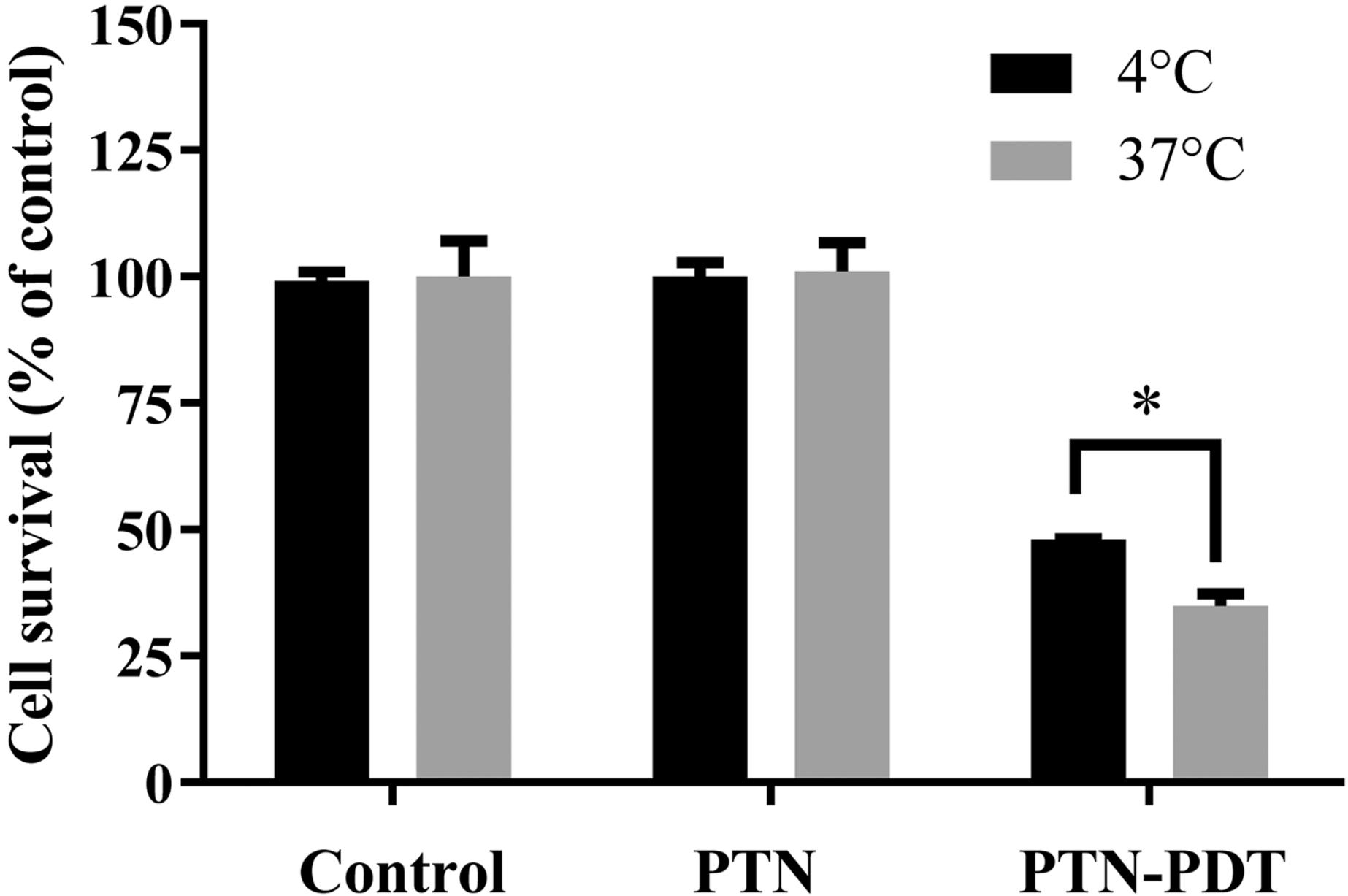
Cell survival (% of control)
150
125
100
75
50
25
0
4°C
37°C
*
Control
PTN
PTN-PDT

Figure 5

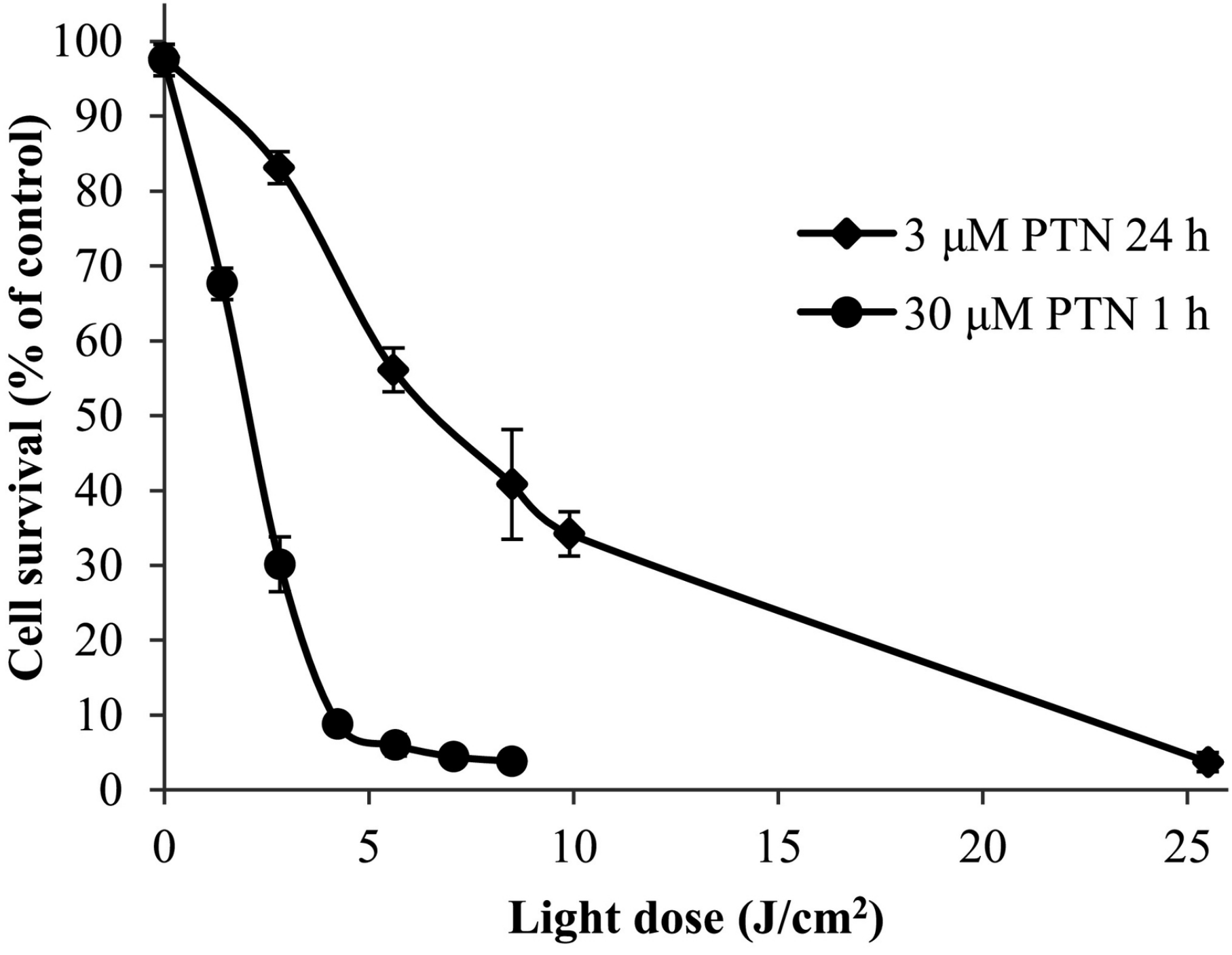
100
90
80
70
60
50
40
30
20
10
0
Cell survival (% of control)
0
5
10
15
20
25
Light dose (J/cm²)
3 μM PTN 24 h
30 μM PTN 1 h

Figure 6

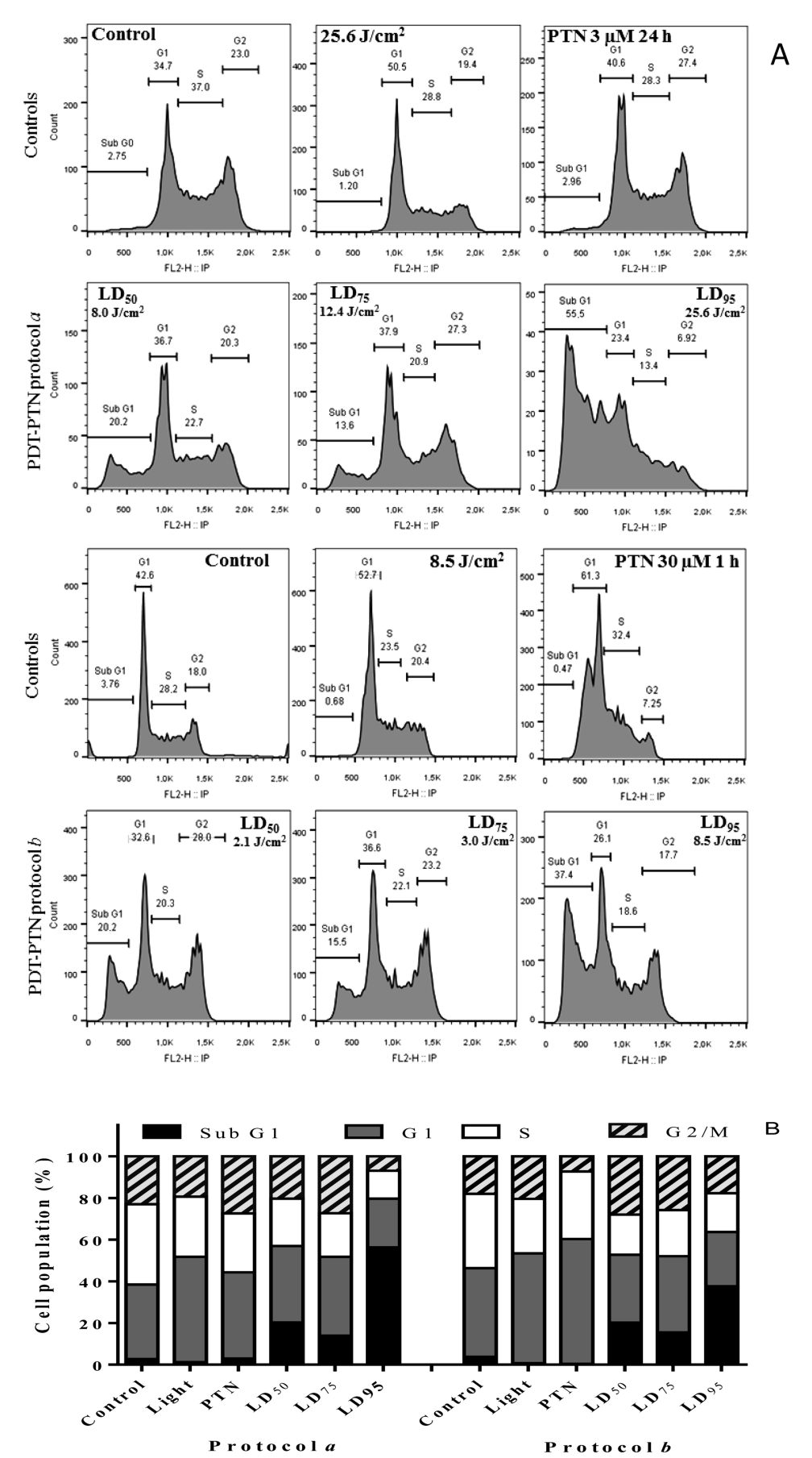
A
Controls
PDT-PTN protocol a
PDT-PTN protocol b
Control
25.6 J/cm²
PTN 3 µM 24 h
LD50 8.0 J/cm²
LD75 12.4 J/cm²
LD95 25.6 J/cm²
8.5 J/cm²
PTN 30 µM 1 h
LD50 2.1 J/cm²
LD75 3.0 J/cm²
LD95 8.5 J/cm²
Count
FL2-H :: IP
B
Sub G1
G1
S
G2/M
Cell population (%)
Control
Light
PTN
LD50
LD75
LD95
Protocol a
Protocol b

Figure 7

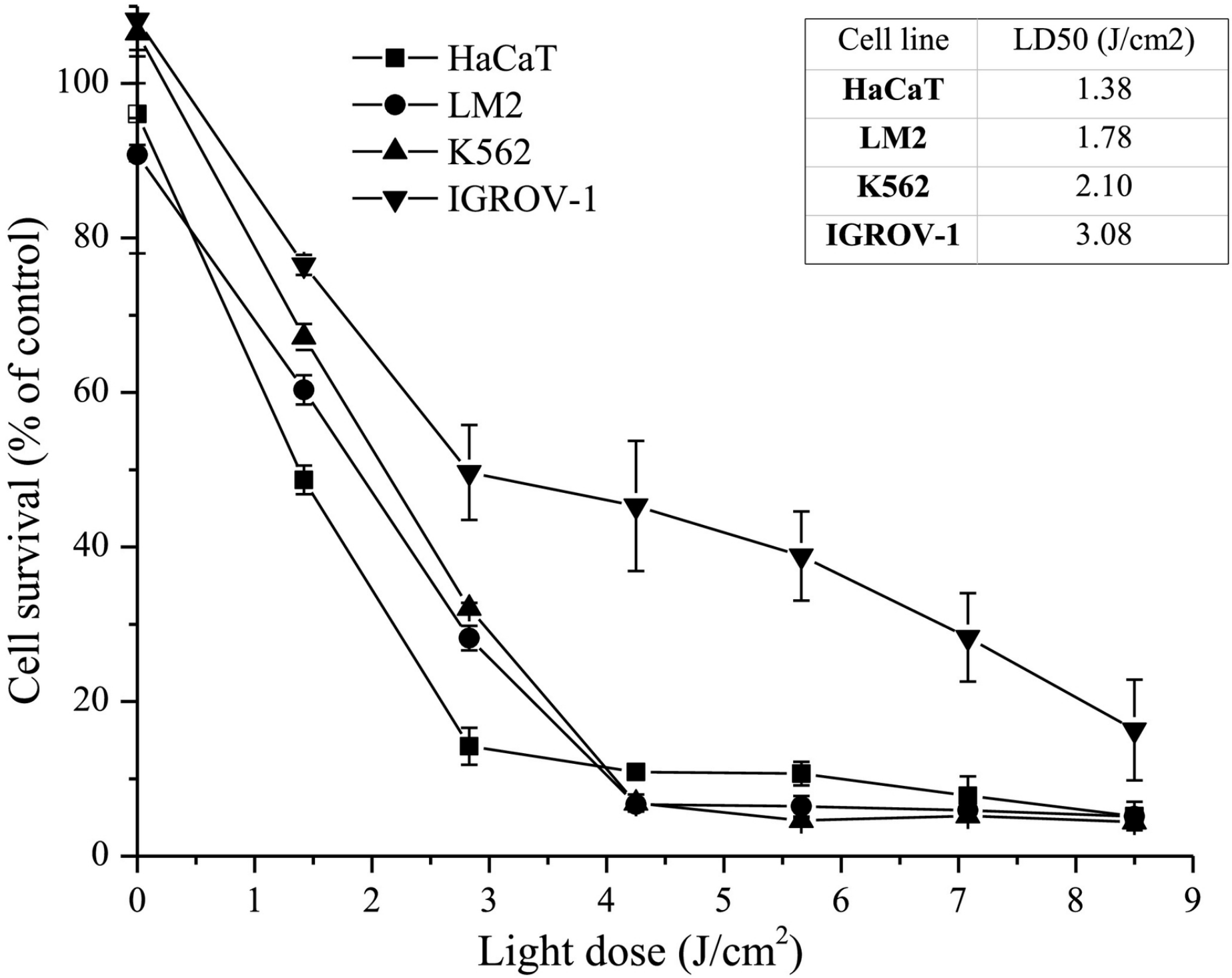

Cell line	LD50 (J/cm2)
HaCaT	1.38
LM2	1.78
K562	2.10
IGROV-1	3.08

Figure 8